which demonstrates that ζ was ubiquitinated. Unmodified ζ (16 kD) was not recognized by the anti-ubiquitin reagents.

The presence of additional activation-dependent species on ubiquitin blots (Fig. 3, A and B) suggested the possibility that other TCR components were ubiquitinated. Immunoprecipitated TCRs were resolved on lower percentage polyacrylamide gels and immunoblotted with anti-ubiquitin (Fig. 4, A and B). Spots that varied in pI and migrated at 34 and 42 kD (Fig. 4B) were suggestive of ubiquitination of the 26-kD CD3 δ subunit, which exhibits heterogeneity in pI as a result of variable modifications with sialic acid. A duplicate immunoblot from activated cells was probed with a polyclonal antiserum to CD3 δ (*18*). In addition to the 26-kD δ, two sets of larger molecular size forms were seen (Fig. 4C) that comigrated with the species detected by anti-ubiquitin (Fig. 4B). These larger forms of δ were detected only in activated cells (Fig. 5A). The presence of charge heterogeneity for ubiquitinated δ indicated that these subunits contained sialic acid and therefore had traversed the intermediate Golgi apparatus.

The finding of relatively acidic species, including a 27-kD form above 21-kD phosphorylated ζ (Fig. 1D) (*10*), indicated that ubiquitinated forms of phosphorylated ζ also exist. To confirm this, we incubated immunoprecipitates from activated and unactivated cells with alkaline phosphatase before electrophoresis on SDS-PAGE (Fig. 5B). This resulted in the loss of phosphorylated ζ (21 kD) as well as the loss of the 27-kD species. Thus, it is apparent that this 27-kD form was ubiquitinated phosphorylated ζ.

We estimate that approximately 10% of TCR-associated ζ is ubiquitinated upon activation. On the basis of the distribution of heterodimers on diagonal gels, it would appear that ubiquitinated ζ chains are more likely to be dimerized to other ubiquitinated ζ molecules than to 16-kD ζ. These proteins exist primarily as components of assembled receptors (Fig. 2) (*10*), and their appearance is not a result of redistribution from a detergent insoluble pool (*10*). Human T cells also demonstrate the same activation-induced forms of ubiquitinated ζ (*10*).

In 2B4 cells, both ubiquitinated ζ and phosphorylated ζ appear within 5 min of stimulation and persist for at least 2 hours (*10*). A dichotomy is apparent in freshly isolated normal splenocytes where ubiquitination of ζ increases markedly with receptor engagement, whereas tyrosine phosphorylated ζ is present at maximal levels without stimulation. This may be a result of the in vivo signals that regulate these processes. Alternatively, it may be a manifestation of differences in the half-lives of these modifications or of the receptors that are altered. The activation-induced ubiquitination of the TCR suggests the possibility of a more generalized function of this process in the regulation of transmembrane receptor function. Ubiquitination may serve as a means to down-regulate receptors by targeting them for degradation, or, like phosphorylation, it may affect function by altering signal transducing properties and associations of modified receptors.

Note added in proof: Ligand-induced changes in the ubiquitination of the receptor for PDGF have recently been described (*19*).

REFERENCES AND NOTES

1. A. M. Weissman, J. S. Bonifacino, R. D. Klausner, L. E. Samelson, J. J. O'Shea, *Year Immunol.* **4**, 74 (1989); J. D. Ashwell and R. D. Klausner, *Annu. Rev. Immunol.* **8**, 139 (1990).
2. L. E. Samelson, J. B. Harford, R. D. Klausner, *Cell* **43**, 223 (1985).
3. H. C. Oettgen *et al.*, *Nature* **320**, 272 (1986); A. M. Weissman, L. E. Samelson, R. D. Klausner, *ibid.* **324**, 480 (1986).
4. L. E. Samelson *et al.*, *Cell* **46**, 1083 (1986).
5. M. Baniyash, P. Garcia-Morales, E. Luong, L. E. Samelson, R. D. Klausner, *J. Biol. Chem.* **263**, 18225 (1988).
6. S. Koyasu *et al.*, *ibid.* **267**, 3375 (1992).
7. S. J. Frank *et al.*, *ibid.*, p. 13656.
8. S. M. Hedrick *et al.*, *Cell* **30**, 141 (1982).
9. O. Leo, M. Foo, D. H. Sachs, L. E. Samelson, J. A. Bluestone, *Proc. Natl. Acad. Sci. U.S.A.* **84**, 1374 (1987).
10. C. Cenciarelli, D. Hou, A. M. Weissman, unpublished data.
11. A. Ciechanover, H. Gonen, S. Elias, A. Mayer, *New Biol.* **2**, 227 (1990).
12. D. Finley and V. Chau, *Annu. Rev. Cell Biol.* **7**, 25 (1991).
13. S. Vijay-Kumar *et al.*, *J. Biol. Chem.* **262**, 6396 (1987); M. Scheffner *et al.*, *Cell* **63**, 1129 (1990); M. Glotzer, A. W. Murray, M. W. Kirschner, *Nature* **349**, 132 (1991); M. Hochstrasser, M. J. Ellison, V. Chau, A. Varshavsky, *Proc. Natl. Acad. Sci. U.S.A.* **88**, 4606 (1991); A. Ciechanover *et al.*, *ibid.*, p. 139.
14. K. G. Murti, H. T. Smith, V. A. Fried, *Proc. Natl. Acad. Sci. U.S.A.* **85**, 3019 (1988).
15. H. Mori, J. Kondo, Y. Ihara, *Science* **235**, 1641 (1987).
16. M. Siegelman *et al.*, *ibid.* **231**, 823 (1986); Y. Yarden *et al.*, *Nature* **323**, 226 (1986); D. W. Leung *et al.*, *ibid.* **330**, 537 (1987).
17. V. A. Fried and H. T. Smith, *Prog. Clin. Biol. Res.* **317**, 733 (1989).
18. L. E. Samelson *et al.*, *J. Immunol.* **137**, 3254 (1986).
19. S. Mori, C.-H. Heldin, L. Claesson-Welsh, *J. Biol. Chem.* **267**, 6429 (1992).
20. J. Kappler, J. White, D. Wegmann, E. Mustain, P. Marrack, *Proc. Natl. Acad. Sci. U.S.A.* **79**, 3604 (1982).
21. M. D. Patel, L. E. Samelson, R. D. Klausner, *J. Biol. Chem.* **262**, 5831 (1987).
22. L. E. Samelson, R. N. Germain, R. H. Schwartz, *Proc. Natl. Acad. Sci. U.S.A.* **80**, 6972 (1983).
23. A. M. Weissman *et al.*, *Science* **239**, 1018 (1988); D. G. Orloff, S. J. Frank, F. A. Robey, A. M. Weissman, R. D. Klausner, *J. Biol. Chem.* **264**, 14812 (1989).

24. Supported by the Howard Hughes Medical Institute–NIH Research Scholars Program (D.H.) and a Cancer Research Institute grant (D.L.W.). For helpful discussions and review of this manuscript, we thank J. D. Ashwell, J. Bonifacino, R. E. Gress, P. A. Henkart, R. D. Klausner, L. E. Samelson, A. Singer, and J. D. Weissman.

19 March 1992; accepted 24 June 1992

The Skeletal Muscle Chloride Channel in Dominant and Recessive Human Myotonia

Manuela C. Koch, Klaus Steinmeyer, Claudius Lorenz, Kenneth Ricker, Friedrich Wolf, Michael Otto, Barbara Zoll, Frank Lehmann-Horn, Karl-Heinz Grzeschik, Thomas J. Jentsch*

Autosomal recessive generalized myotonia (Becker's disease) (GM) and autosomal dominant myotonia congenita (Thomsen's disease) (MC) are characterized by skeletal muscle stiffness that is a result of muscle membrane hyperexcitability. For both diseases, alterations in muscle chloride or sodium currents or both have been observed. A complementary DNA for a human skeletal muscle chloride channel (*CLC*-1) was cloned, physically localized on chromosome 7, and linked to the T cell receptor β (*TCRB*) locus. Tight linkage of these two loci to GM and MC was found in German families. An unusual restriction site in the *CLC*-1 locus in two GM families identified a mutation associated with that disease, a phenylalanine-to-cysteine substitution in putative transmembrane domain D8. This suggests that different mutations in *CLC*-1 may cause dominant or recessive myotonia.

Autosomal recessive generalized myotonia (GM) is a nondystrophic disorder of skeletal muscle and was clinically separated (*1*) from autosomal dominant myotonia congenita (MC) (*1*, *2*). In GM, myotonic stiffness starts in early childhood in the legs. It progresses for some years, affecting the arms, neck, and facial muscles. After the patient reaches approximately 20 years of age, the disease remains unchanged. In most patients, muscle stiffness is associated with transient weakness after rest. In MC, complaints are similar but more benign.

Muscle stiffness caused by these diseases is a result of repetitive firing of muscle fiber action potentials (myotonic runs) (*3*). Two mechanisms have been proposed to cause the underlying intrinsic muscle hyperexcitability: (i) a decrease in muscle chloride conductance, as found in several human

muscle fibers analyzed electrophysiologically in vitro (*4*–*6*) and (ii) alterations of sodium channel activity. In support of the first, a genetic defect in the skeletal muscle Cl^- channel CLC-1 (*7*) was recently found in the recessive myotonic mouse mutant ADR (*8*). Because Cl^- conductance accounts for about 80% of normal resting muscle membrane conductance (*9*), its decrease [or pharmacological blockage (*3*, *9*)] leads to a slower rate of repolarization after action potentials and to myotonic runs. Alterations of Na^+ channel activity, especially late openings, were observed in a large proportion of biopsies from GM patients (*4*, *10*) and especially in biopsies from MC patients (*11*). Related findings were made with other disorders with the symptom myotonia, such as myotonic dystrophy (*10*, *12*) and Schwarz-Jampel syndrome (*13*).

By homology screening with the major rat skeletal muscle chloride channel CLC-1 (*7*), we cloned a partial human CLC-1 cDNA that covers about 80% of the coding sequence (*14*). This region is 88% identical to the rat channel in amino acids (*14*). CLC-1 was then physically localized by somatic cell hybrids to the chromosomal region 7q32-qter (Fig. 1) and used to search for restriction fragment length polymorphisms (RFLPs) in ten unrelated individuals. Among 25 enzymes tested, diallelic Nsi I and Ava II RFLPs were revealed (*15*) and subsequently used in five reference pedigrees to prove linkage to the T cell receptor β (*TCRB*) locus (*16*) on chromosome 7q. Tight linkage with no recombinants was shown for CLC-1/Nsi I versus CLC-1/Ava II with a lod (logarithm of odds) score (*17*) of $z = 3.62$ at a recombination fraction of $\theta = 0.0$ and for *TCRB* versus the combined CLC-1 haplotype of $z = 5.23$ at $\theta = 0.0$ (Table 1). The fact that the CLC-1 locus was previously linked to the *TCRB* locus in mice (*8*) supports the mouse-human homology map for this chromosomal region on human chromosome 7q and mouse chromosome 6.

Both human gene probes, CLC-1 and *TCRB*, were used to test the members of seven GM families (*18*). Linkage was shown to the CLC-1 haplotype ($z = 4.69$ at $\theta = 0.0$) and to a lesser extent to *TCRB* ($z = 2.53$ at $\theta = 0.0$). Combined linkage analysis of GM to both loci resulted in a maximum multipoint lod score of $z = 5.79$ at $\theta = 0.0$ (Table 1).

In addition, for two of the clinically typical GM families, a rare Nsi I pattern was detected with the CLC-1 probe. In pedigree 4003 (Fig. 2), the consanguineous parents show this unusual Nsi I pattern (A3). They both lack the ≈17-kb fragment of allele A2, which is replaced by ≈10- and ≈7-kb fragments as a result of the additional Nsi I site. The three affected sons are homozygous for this site. In one other family, only the father was a carrier for A3 and transmitted it to all three affected offspring (*19*). Because this unusual Nsi I site was not observed in 110 control individuals, this suggests that it may be generated directly by the disease-causing mutation. We identified this mutation using restriction by Nsi I to search for it in genomic CLC-1 clones isolated from libraries constructed from an unaffected individual and from a GM patient homozygous for this site (one of the affected brothers of pedigree 4003) (Fig. 2) (*20*). Sequencing revealed a T-to-G exchange in exonic sequence (Fig. 3A), leading to the Nsi I site

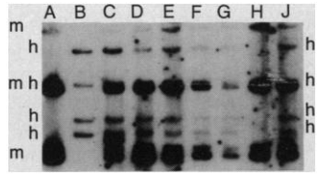

Fig. 1. Localization of the human *CLC*-1 gene on chromosome 7. Blot hybridization pattern of Eco RI–digested DNAs from a panel of chromosome 7–specific, human-mouse somatic cell hybrids (*26*) with *CLC*-1 cDNA. Lane A, total mouse DNA (m, mouse-specific bands); lane B, total human DNA (h, four human-specific bands); lane C, hybrid with entire human chromosome 7 (5387-3c110); lane D, hybrid ITA9-2-21-14 (human chromosome 7p14-qter); lane E, hybrid RuRag6-19 (human chromosome 7cen-qter); lane F, hybrid GM2068Rag22-2 (human chromosome 7q22-qter); lane G, hybrid GM1059Rag5, and lane J, hybrid 7851Rag10-1, both with an interstitial deletion of human chromosome 7q22-7q32; and lane H, hybrid 194Rag6-13-3 (human chromosome 7pter-7q32). A human signal is lacking in lane H, which thus localizes the probe to the chromosomal region 7q32-qter.

Table 1. Lod scores (*z* values) for linkage of *CLC*-1 and chromosome 7 marker *TCRB* to GM and MC. Because the two *CLC*-1 RFLPs Nsi I and Ava II were shown to be linked with no recombinants, they were treated as a single marker for linkage analysis to GM and MC and were labeled *CLC*-1 haplotype.

Linkage comparison	Recombination fraction (θ)							
	0.000	0.001	0.01	0.05	0.1	0.2	0.3	0.4
CLC-1/Nsi I versus *CLC*-1/Ava II	3.62	3.61	3.52	3.22	2.83	2.03	1.22	0.48
TCRB versus *CLC*-1 haplotype	5.23	5.21	5.07	4.49	3.76	2.34	1.10	0.28
GM versus *CLC*-1 haplotype	4.69	4.67	4.57	4.10	3.50	2.29	1.15	0.31
GM versus *TCRB*	2.53	2.52	2.45	2.16	1.81	1.13	0.56	0.15
GM versus *TCRB/CLC*-1 haplotype	5.79	5.77	5.61	5.00	4.23	2.72	1.35	0.36
MC versus *CLC*-1 haplotype	2.75	2.74	2.66	2.33	1.92	1.18	0.58	0.16
MC versus *TCRB*	3.42	3.41	3.33	2.97	2.54	1.71	0.94	0.33
MC versus *TCRB/CLC*-1 haplotype	4.58	4.57	4.47	4.00	3.43	2.28	1.26	0.44

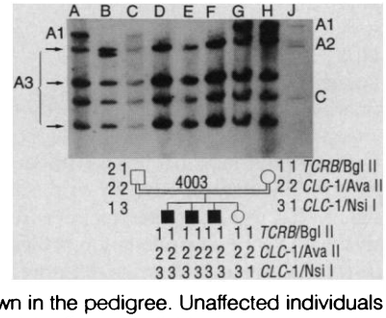

Fig. 2. Southern hybridization analysis of Nsi I–digested DNA with the *CLC*-1 gene probe from two control individuals affected with GM (lanes A and B), GM family 4003 (lanes C through H), and an unaffected control person (lane J). A1 = allele 1, >30 kb; A2 = allele 2 (doublet), ≈21 kb and ≈17 kb; C = constant band, ≈8 kb. The arrows indicate the unusual Nsi I pattern (A3) with fragments of ≈21 kb, ≈10 kb, and ≈7 kb. Affected individuals in lanes D through F are thus homozygous for A3, whereas affected individuals in lanes A and B are heterozygous for alleles A1 and A3 and for A2 and A3, respectively. Haplotypes for *CLC*-1 and the closely linked gene probe *TCRB* are shown in the pedigree. Unaffected individuals are presented as empty circles (female) and a square (male); affected individuals are represented by filled symbols. Symbols are shown below the corresponding Southern lane.

M. C. Koch, F. Wolf, M. Otto, K.-H. Grzeschik, Medical Center for Human Genetics, Marburg University, Bahnhofstrasse 7a, D-3550 Marburg, Germany.
K. Steinmeyer, C. Lorenz, T. J. Jentsch, Center for Molecular Neurobiology (ZMNH), Hamburg University, Martinistrasse 52, D-2000 Hamburg 20, Germany.
K. Ricker, Clinical Neurology, Würzburg University, Josef-Schneider-Strasse 11, D-8700 Würzburg, Germany.
B. Zoll, Institute for Human Genetics, Göttingen University, Goßlerstrasse 12d, D-3400 Göttingen, Germany.
F. Lehmann-Horn, Clinical Neurology, Technical University, Möhlstrasse 28, D-8000 Munich, Germany.
*To whom correspondence should be addressed.

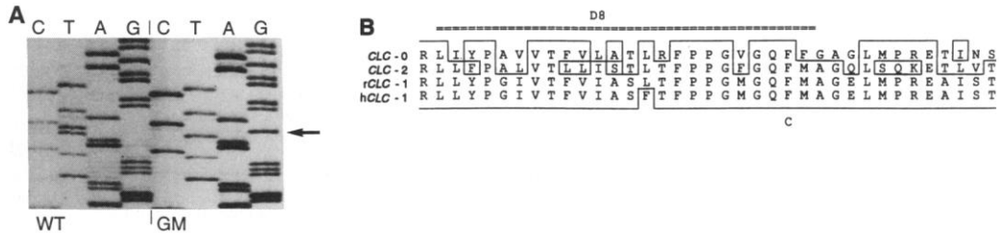

Fig. 3. Identification of a mutation present in GM. (**A**) Autoradiographs of sequencing gels that show the region of interest. WT, genomic *CLC*-1 clone from an unaffected individual; GM, genomic clone from a patient homozygous for this GM mutation. The arrow indicates the T-to-G exchange [at equivalent position 1238 in the rat *CLC*-1 cDNA (*7*)], leading to the observed Nsi I site (ATGCAT) and to a Phe-to-Cys exchange (at equivalent position 413 in the rat channel protein). (**B**) Homology between different members of the voltage-gated Cl^- channel family in the region affected by the mutation. *CLC*-0, *Torpedo marmorata* electric organ Cl^- channel (*23*); *CLC*-2, ubiquitous rat Cl^- channel (*24*); r*CLC*-1, rat skeletal muscle Cl^- channel (*7*); h*CLC*-1, human skeletal muscle Cl^- channel (sequenced at both the genomic and the cDNA levels). Identical residues are boxed. The dashes denote putative membrane-spanning domain D8, and the C at the bottom indicates the mutation found in GM. Abbreviations for the amino acid residues are: A, Ala; C, Cys; D, Asp; E, Glu; F, Phe; G, Gly; H, His; I, Ile; K, Lys; L, Leu; M, Met; N, Asn; P, Pro; Q, Gln; R, Arg; S, Ser; T, Thr; V, Val; W, Trp; and Y, Tyr.

and to a predicted Phe-to-Cys exchange. This Phe, located toward the end of putative membrane span D8, is highly conserved among different members of the voltage-gated Cl^- channel family and thus is probably important for channel function (Fig. 3B). The propensity of the new Cys to form improper disulfide bonds may be involved in the pathogenic effect of this mutation.

Thus, there is strong evidence that GM is caused by defects in the skeletal muscle Cl^- channel CLC-1. Definitive proof that the Phe-to-Cys mutation really causes the disease will have to await the functional expression of the mutated channel. Because this mutation is present in only a proportion of affected GM individuals, there is probably heterogeneity in CLC-1 mutations that cause GM.

Having shown close linkage of CLC-1 to the disorder GM and having identified a GM-associated mutation, we tested the members of four MC families (*18*) for the same linkage hypothesis (Fig. 4). The MC data resulted in a maximum multipoint lod score of $z = 4.58$ at $\theta = 0.0$ (12 scorable meioses) (Table 1), which suggests that CLC-1 is also involved in this dominant disease. Definitive proof will require the identification of CLC-1 mutations in MC.

Recent reports have stressed the effects of altered Na^+ channel kinetics (*11*) in MC. These kinetic effects are likely to be secondary, especially because similar observations were made in myotonic dystrophy (*10, 12*), where the defective gene has been mapped to chromosome 19 (*21*) and whose gene product is probably a protein kinase (*22*).

Thus, our data suggest that mutations in the muscle Cl^- channel can cause myotonia with either a recessive or a dominant mode of inheritance. A recessive form is easily explained by a total loss of function. This has been described in ADR mice (*8*), which we now show to be an excellent model system for human myotonia. On the other hand, a mutation acting dominantly could possibly be explained by a homomultimeric structure of the channel [the multimeric state of channels of this family is currently unknown (*7, 23, 24*)]. In this model, the channel subunit encoded by the mutated gene associates with and inactivates the functional subunits encoded by the normal allele. Such a situation was found with transgenic *Drosophila* that expresses a mutant *Shaker* K^+ channel (*25*). This model may also fit with the observation that the clinical phenotype is often less severe in MC than in GM patients (*1*) and that electrophysiological evidence for reduced Cl^- conductance was weaker in MC (*11*); possibly, some of the channel complexes escape inactivation by the mutated subunit. Thus, our work also indirectly suggests a multimeric structure of CLC-1 Cl^- channels.

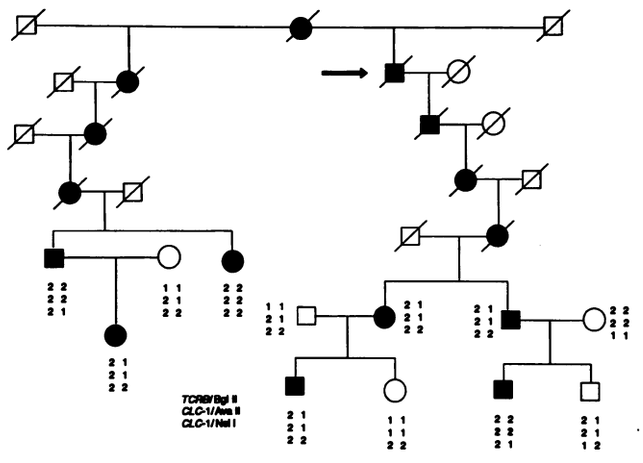

Fig. 4. Pedigree of the Thomsen family [arrow indicates J. Thomsen, who first described MC (*2*)], showing the genotypes for the closely linked gene probes *TCRB* and *CLC*-1, generating a multipoint lod score of $z = 2.15$ at $\theta = 0.0$. The design of the pedigree has been changed (birth order and sex) to protect patient confidentiality. Symbols are as in Fig. 2.

REFERENCES AND NOTES

1. P. E. Becker, *Myotonia Congenita and Syndromes Associated with Myotonia* (Thieme, Stuttgart, 1977).
2. J. Thomsen, *Arch. Psychiatr. Nervenkrankh.* **6**, 702 (1876).
3. R. Rüdel and F. Lehmann-Horn, *Physiol. Rev.* **65**, 310 (1985).
4. C. Franke *et al.*, *Muscle Nerve* **14**, 762 (1991).
5. R. J. Lipicky, S. H. Bryant, J. H. Salmon, *J. Clin. Invest.* **50**, 2091 (1971).
6. R. Rüdel, K. Ricker, F. Lehmann-Horn, *Muscle Nerve* **11**, 202 (1988).
7. K. Steinmeyer, C. Ortland, T. J. Jentsch, *Nature* **354**, 301 (1991).
8. K. Steinmeyer *et al.*, *ibid.*, p. 304.
9. A. H. Bretag, *Physiol. Rev.* **67**, 618 (1987).
10. R. Rüdel, J. P. Ruppersberg, W. Spittelmeister, *Muscle Nerve* **12**, 281 (1989).
11. P. A. Iaizzo *et al.*, *Neuromusc. Disorder* **1**, 47 (1991).
12. C. Franke, H. Hatt, P. A. Iaizzo, F. Lehmann-Horn, *J. Physiol. (London)* **425**, 391 (1990).
13. F. Lehmann-Horn *et al.*, *Muscle Nerve* **13**, 528 (1990).
14. A ^{32}P-labeled rat *CLC*-1 cDNA (*7*), extending from bp 970 to bp 1881, was used to screen a human skeletal muscle cDNA library in λZAPII (Stratagene) at moderately high stringency (45% formamide, ×5 saline sodium citrate, ×5 Denhardt's, and 0.1% SDS at 42°C). A single positive clone was identified and subcloned by in vivo excision. Sequencing revealed that it begins at bp 510 relative to the rat channel and extends into the 3′ noncoding region (total length = 2517 bp) (K. Steinmeyer, C. Lorenz, T. J. Jentsch, in preparation). The sequence has been deposited in the European Molecular Biology Laboratory/GenBank database (accession number M97820). Comparison to the rat *CLC*-1 sequence by the AALIGN program (DNASTAR) revealed that it is 88% homologous to that channel.
15. For Nsi I, the allele sizes and frequencies (110 unrelated Caucasians) were A1 > 30 kb (0.6) and A2 ≈21 kb and ≈17 kb (0.4), and for Ava II (90 unrelated individuals) were A1 ≈15 kb (0.2) and A2 ≈12 kb (0.8).
16. Bgl II reveals a two-allele polymorphism in the *TCRB* locus [Y. Yanagi *et al.*, *Nature* **308**, 145 (1984)] (A1 ≈10.0 kb and A2 ≈9.5 kb; frequencies = 0.55 and 0.45).
17. Lod scores (z = maximum log likelihood ratio, θ = recombination fraction) were calculated with the LINKAGE computer program package (version 5.04, updated by J. Ott). For GM, an autosomal

recessive and for MC an autosomal dominant inheritance with 100% penetrance were assumed (all unaffected individuals were beyond the age of risk). The prevalence of these two diseases was assumed (*1*) to be 1:50,000 in GM and 1:23,000 in MC.

18. After receipt of informed consent, seven families (a total of 14 affected and 13 nonaffected siblings) with the diagnosis of GM and 4 families with MC (20 affected, 7 nonaffected, and 7 spouses) were studied. The age of onset for individuals with GM was 2 to 10 years, and 1 to 18 years for MC. All individuals in a family received a thorough neurological examination. In addition, a standardized forearm cooling test was performed on MC individuals to exclude paramyotonia congenita [K. Ricker *et al.*, *Arch. Neurol.* **47**, 268 (1990)]. For the purpose of the study, it was assumed that GM and MC are single-gene disorders, where variation in symptoms probably results from different mutations in the same locus.
19. M. C. Koch *et al.*, data not shown.
20. A genomic library in λFIXII was constructed with lymphocyte DNA from a GM patient homozygous for the unusual Nsi I site (Fig. 2), and another genomic human library in λFIXII was purchased (Stratagene). Phages hybridizing to human *CLC*-1 cDNAs were purified, and their inserts were isolated, digested with Nsi I, and subcloned into pGem5Zf. The Nsi I fragment of interest was identified by hybridization to successively smaller cDNA fragments that still recognized the unusual Nsi I site detected by genomic Southern (DNA) analysis, and the region surrounding the restriction site was sequenced with the chain termination method. The sequences shown in Fig. 3 were obtained by means of internal sequencing primers located in the intron preceding the D8 coding sequence.
21. H. Eiberg *et al.*, *Clin. Genet.* **24**, 159 (1983); H. G. Harley *et al.*, *Am. J. Hum. Genet.* **49**, 68 (1991).
22. J. D. Brook *et al.*, *Cell* **68**, 799 (1992); Y.-H. Fu *et al.*, *Science* **255**, 1256 (1992).
23. T. J. Jentsch, K. Steinmeyer, G. Schwarz, *Nature* **348**, 510 (1990); C. K. Bauer, K. Steinmeyer, J. R. Schwarz, T. J. Jentsch, *Proc. Natl. Acad. Sci. U.S.A.* **88**, 11052 (1991).
24. A. Thiemann, S. Gründer, M. Pusch, T. J. Jentsch, *Nature* **356**, 57 (1992).
25. S. Gisselmann *et al.*, *EMBO J.* **8**, 2359 (1989).
26. A. Jobs *et al.*, *Hum. Genet.* **84**, 147 (1990).
27. We thank G. Grahmann and C. Schmekal for technical assistance, L. C. Tsui for the *TCRB* gene probe, and all families for their collaboration. Supported by grants from the Deutsche Forschungs-gemeinschaft (M.C.K. and T.J.J.), the Bundesministerium für Forschung und Technologie (T.J.J.), the Muscular Dystrophy Association (T.J.J.), and the Deutsche Gesellschaft Bekämpfung der Muskelkrankheiten.

12 March 1992; accepted 17 June 1992

Hypovirulence of Chestnut Blight Fungus Conferred by an Infectious Viral cDNA

Gil H. Choi and Donald L. Nuss*

Strains of the chestnut blight fungus *Cryphonectria parasitica* that contain viral double-stranded RNAs often exhibit reduced virulence. Such hypovirulent strains act as biocontrol agents by virtue of their ability to convert virulent strains to hypovirulence after anastomosis. Transformation of virulent *C. parasitica* strains with a full-length complementary DNA copy of a hypovirulence-associated viral RNA conferred the complete hypovirulence phenotype. Cytoplasmic double-stranded RNA was resurrected from the chromosomally integrated complementary DNA copy and was able to convert compatible virulent strains to hypovirulence. These results establish viral double-stranded RNA as the causal agent of hypovirulence and demonstrate the feasibility of engineering hypovirulent fungal strains.

The North American chestnut blight epidemic, initiated by the unintentional introduction of the Asian fungus *Cryphonectria (Endothia) parasitica* at the turn of the century, resulted in the destruction of several billion mature American chestnut trees (*1–4*). The potential for biological control of chestnut blight effected by naturally occurring strains of C. *parasitica* that exhibit reduced levels of virulence (hypovirulence) has been demonstrated (*5–7*). Whereas virulent C. *parasitica* strains penetrate and destroy bark and cambium layers and cause wilting and death, hypovirulent strains usually produce superficial cankers that eventually heal. Hypovirulence is correlated with the presence of cytoplasmically replicating unencapsidated double-stranded RNAs (dsRNAs) (*8*). The ability of these genetic elements and the hypovirulence phenotype to be transmitted to virulent fungal strains after anastomosis (physical fusion of hyphae) provides the basis for disease control (*7*).

The largest dsRNA present in hypovirulent C. *parasitica* strain EP713, large dsRNA (L-dsRNA), was recently cloned and characterized (*9–12*). The similarity of the L-dsRNA genetic organization and expression strategy to those of several viral genomes (*11*) and an apparent evolutionary relationship to the plant potyviruses (*13*) prompted the introduction of the term hypovirulence-associated virus (HAV) to denote this class of genetic elements (*11*). Efforts to rigorously demonstrate HAV dsRNAs as the causal agent of hypovirulence have been hampered by the inability of these viral elements to initiate infection by an extracellular route, a common property of mycoviruses and fungus-associated unencapsidated viral-like RNAs (*14–16*). We describe the construction of a full-length cDNA clone of EP713 L-dsRNA that, when introduced into virulent C. *parasitica* strains by DNA-mediated transformation, generated a resurrected, cytoplasmically replicating dsRNA form from the integrated cDNA copy.

One strand of L-dsRNA contains a 3′ polyadenylate [poly(A)] tail that is base-paired to a stretch of polyuridine [poly(U)] present at the 5′ terminus of the complementary strand (*17*). The molecule consists of 12,712 bp, excluding the poly(A):poly(U) homopolymer domain and contains two large open reading frames (ORF) within the poly(A) strand that were designated ORF A (622 codons) and ORF B (3,165 codons) (*11*). To construct a full-length cDNA clone of L-dsRNA, we first generated several large intermediate clones from a set of overlapping partial cDNA clones (Fig. 1). A four-factor ligation-transformation was then performed to generate plasmid pLDST that contained a full-length cDNA copy of L-dsRNA inserted between the Xba I and Hind III sites of pUC19. Unique Ssp I and Spe I sites were intro-

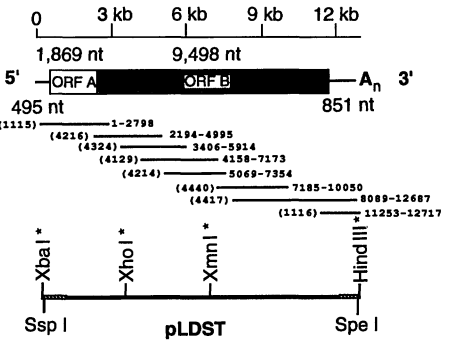

Fig. 1. Genetic organization of the hypovirulence-associated virus RNA, L-dsRNA, present in hypovirulent *C. parasitica* strain EP713 [American Type Culture Collection (ATCC) number 52571] and construction of the full-length cDNA clone pLDST. The general organization of the coding sense strand of L-dsRNA is indicated at the top; overlapping cDNA clones that span the entire molecule are represented by the horizontal lines below. Clone designations are indicated at the left of each line, and the map coordinates (*11*) covered by each clone are indicated to the right of each line. Modifications of the terminal regions of the L-dsRNA cDNA (indicated by diagonal stripes in pLDST) included the addition of Xba I and Ssp I sites at the 5′ terminus and a 22-residue-long stretch of poly(A):poly(U) to simulate the natural homopolymer tail followed by Spe I and Hind III sites at the 3′ terminus. Restriction sites used in the four-factor ligation to form pLDST are indicated by an asterisk.

Department of Molecular Oncology and Virology, Roche Institute of Molecular Biology, Roche Research Center, Nutley, NJ 07110.

*To whom correspondence should be addressed.